Biochemical and Biophysical Research Communications 424 (2012) 451–455

Contents lists available at SciVerse ScienceDirect

Biochemical and Biophysical Research Communications

journal homepage: www.elsevier.com/locate/ybbrc

Pseudo-enzymatic hydrolysis of 4-nitrophenyl acetate by human serum albumin: pH-dependence of rates of individual steps

Paolo Ascenzi [a,b,*], Magda Gioia [c,d], Gabriella Fanali [e], Massimo Coletta [c,d], Mauro Fasano [e]

[a] Interdepartmental Laboratory of Electron Microscopy, University Roma Tre, Via della Vasca Navale 79, I-00146 Roma, Italy
[b] National Institute of Biostructures and Biosystems, Viale Medaglie d'Oro 305, I-00136 Roma, Italy
[c] Department of Clinical Sciences and Translational Medicine, University of Roma "Tor Vergata", Via Montpellier 1, I-00133 Roma, Italy
[d] Interuniversity Consortium for the Research on the Chemistry of Metals in Biological Systems, Via Celso Ulpiani 27, I-70126 Bari, Italy
[e] Department of Theoretical and Applied Sciences, Division of Biomedical Research, University of Insubria, Via Alberto da Giussano 12, I-21052 Busto Arsizio (VA), Italy

ARTICLE INFO

Article history:
Received 22 June 2012
Available online 4 July 2012

Keywords:
Human serum albumin
4-Nitrophenyl acetate
Pre-steady-state kinetics
Steady-state kinetics
pH effects

ABSTRACT

Human serum albumin (HSA) displays esterase activity reflecting multiple irreversible chemical modifications rather than turnover. Here, kinetics of the pseudo-enzymatic hydrolysis of 4-nitrophenyl acetate (NphOAc) are reported. Under conditions where [HSA] $\geqslant 5\times$[NphOAc] and [NphOAc] $\geqslant 5\times$[HSA], the HSA-catalyzed hydrolysis of NphOAc is a first-order process for more than 95% of its course. From the dependence of the apparent rate constants k_{app} and k_{obs} on [HSA] and [NphOAc], respectively, values of K_s, k_{+2}, and k_{+2}/K_s were determined. Values of K_s, k_{+2}, and k_{+2}/K_s obtained at [HSA] $\geqslant 5\times$[NphOAc] and [NphOAc] $\geqslant 5\times$[HSA] are in good agreement, the deacylation step being rate limiting in catalysis. The pH-dependence of k_{+2}/K_s, k_{+2}, and K_s reflects the acidic pK_a shift of the Tyr411 catalytic residue from 9.0 ± 0.1 in the substrate-free HSA to 8.1 ± 0.1 in the HSA:NphOAc complex. Accordingly, diazepam inhibits competitively the HSA-catalyzed hydrolysis of NphOAc by binding to Tyr411.

1. Introduction

The three-domain organization of HSA is at the root of its capability to bind not only endogenous and exogenous low molecular weight compounds but also peptides and proteins at multiple sites. Remarkably, 35 proteins have been found to be associated to HSA under physiological conditions; the fraction of peptides and proteins bound to HSA has been defined as "albuminome" [1–6].

Upon binding endogenous and exogenous (macro)molecules, HSA undergoes chemical modifications, including acetylation, cysteinylation, homocysteinylation, glutathionylation, glycosylation, glycation, nitrosylation, nitration, oxidation, phosphorylation, biotinylation, and chlorination [6]; remarkably, chemical modifications may affect HSA binding properties and may confer antigenicity properties [1,6,7].

In addition to its reversible and irreversible ligand binding capabilities, HSA displays pseudo-enzymatic properties. In fact, most of the apparent enzymatic properties of HSA (*e.g.*, esterase activity) are the result of multiple irreversible chemical modifications rather than of the catalytic activity occurring at a single reactive site [8]. Remarkably, the apparent HSA-catalyzed hydrolysis of 4-nitrophenyl acetate (NphOAc) is the result of the irreversible acetylation of 82 residues rather than of turnover. In fact, only Tyr411 is acetylated within the first 5 min of reaction with 5.0×10^{-4} M NphOAc; after 30 min to 6 h, the partial acetylation of additional 16–17 residues of HSA takes place, including Asp1, Lys4, Lys12, Tyr411, Lys413, and Lys414. HSA incubation with 1.0×10^{-2} M NphOAc results in the acetylation of 59 Lys, 10 Ser, 8 Thr, 4 Tyr, and 1 Asp [8].

Here, kinetics of the HSA pseudo-enzymatic hydrolysis of NphOAc, obtained under conditions where [HSA] $\geqslant 5\times$[NphOAc] and [NphOAc] $\geqslant 5\times$[HSA] (between pH 5.8 and 10.2, at 22.0 °C), are reported. The pH-dependence of the rates of the individual steps for the HSA pseudo-esterase activity probably depends on the acid–base equilibrium of Tyr411 and parallels the neutral-to-basic allosteric transition. Accordingly, diazepam inhibits competitively the HSA-catalyzed hydrolysis of NphOAc by binding to Tyr411.

2. Materials and methods

HSA, NphOAc, diazepam, 4-nitrophenol (NphOH), bis(2-hydroxyethyl)amino-tris(hydroxymethyl)methane (Bis-Tris), 4-(2-hydroxyethyl)-1-piperazineethanesulfonic acid (Hepes), 3-

Abbreviations: AMPSO, 3-[(1,1-dimethyl-2-hydroxyethyl)amino]-2-hydroxypropanesulfonic acid; Bis-Tris, bis(2-hydroxyethyl)amino-tris(hydroxymethyl)-methane; Hepes, 4-(2-hydroxyethyl)-1-piperazineethanesulfonic acid; HSA, human serum albumin; NphOH, 4-nitrophenol; NphOAc, 4-nitrophenyl acetate.

* Corresponding author at: Interdepartmental Laboratory of Electron Microscopy, University Roma Tre, Via della Vasca Navale 79, I-00146 Roma, Italy. Fax: +39 06 5733 6321.
E-mail address: ascenzi@uniroma3.it (P. Ascenzi).

0006-291X/$ - see front matter © 2012 Elsevier Inc. All rights reserved.
http://dx.doi.org/10.1016/j.bbrc.2012.06.131

[(1,1-dimethyl-2-hydroxyethyl)amino]-2-hydroxypropanesulfonic acid (AMPSO), and 2-amino-2-methyl-1-propanol were obtained from Sigma–Aldrich (St. Louis, MO, USA). All chemicals were of analytical or reagent grade and were used without further purification.

HSA (from Sigma–Aldrich, St. Louis, MO, USA) was essentially fatty acid free, according to the charcoal delipidation protocol [9–11], and was used without further purification. The HSA stock solution ([HSA] = 1.2×10^{-2} M) was prepared by dissolving HSA in 1.0×10^{-2} M phosphate buffer pH 7.0, at 22.0 °C. The HSA concentration was determined spectrophotometrically at 279 nm ($\varepsilon = 3.6 \times 10^4\ M^{-1}\ cm^{-1}$) [1]. Then, the HSA stock solution was diluted in the desired buffer (Bis–Tris buffer, pH 5.8–7.2; Hepes buffer, pH 6.8–8.2; AMPSO buffer, pH 8.3–9.7; 2-amino-2-methyl-1-propanol buffer, pH 9.0–10.2; all 0.1 M), the final pH ranging between 5.8 and 10.2. The final HSA concentration ranged between 4.0×10^{-6} M and 1.6×10^{-3} M.

The NphOAc solution was prepared by dissolving the substrate in a 3.0×10^{-3} M Bis–Tris buffer solution (pH 5.8) in the presence of 10% acetonitrile. The NphOAc concentration was determined spectrophotometrically at 400 nm ($\varepsilon = 1.8 \times 10^4\ M^{-1}\ cm^{-1}$; pH > 8.5 and 22.0 °C), allowing to calculate the amount of 4-nitrophenol released from the substrate [12]. The final NphOAc concentration ranged between 1.0×10^{-5} M and 1.8×10^{-3} M. The final acetonitrile concentration was 0.5% (v/v) [13].

Kinetics and thermodynamics of the HSA-catalyzed hydrolysis of NphOAc were followed spectrophotometrically between 350 nm and 450 nm by mixing the HSA and NphOAc solutions with the SMF-20 rapid-mixing stopped-flow apparatus (Bio-Logic, Claix, France).

Kinetics and thermodynamics of the HSA-catalyzed hydrolysis of NphOAc, obtained under conditions where [NphOAc] ⩾ 5×[HSA] and [HSA] ⩾ 5×[NphOAc], between pH 5.8 and 10.2 and 22.0 °C, were analyzed in the framework of the minimum three step-mechanism reported in Scheme 1 [8,12–15], where HSA is the substrate-free protein, NphOAc is the substrate, HSA:NphOAc is the reversible protein-substrate complex, HSA-OAc is considered to be an ester formed between the acyl moiety of the substrate and the O atom of the Tyr411 phenoxyl group [8], AcOH is acetic acid, k_{+1} is the second-order rate constant for the formation of the HSA:NphOAc complex starting from HSA and NphOAc, k_{-1} is the first-order rate constant for the dissociation of the HSA:NphOAc complex to HSA and NphOAc, K_s ($=k_{-1}/k_{+1}$) is the pre-equilibrium constant, k_{+2} is the first-order acylation rate constant, k_{-2} is the first-order rate constant for the conversion of HSA-OAc to HSA:NphOAc, k_{+3} is the first-order deacylation rate constant, and k_{-3} is the second-order rate constant for the formation of the HSA-OAc adduct starting from HSA and AcOH.

Kinetics and thermodynamics of the HSA-catalyzed hydrolysis of NphOAc, at pH 7.5 and 22.0 °C, were also determined in the presence of diazepam ranging between 1.0×10^{-5} M and 7.7×10^{-5} M. The HSA concentration was 4.0×10^{-6} M and the NphOAc concentration ranged between 1.0×10^{-5} M and 8.0×10^{-5} M[16].

Kinetics and thermodynamics of the HSA pseudo-esterase activity were analyzed using the GraphPad Prism program (GraphPad Software, Inc., La Jolla, CA, USA). The results are given as mean values of at least four experiments plus or minus the corresponding standard deviation.

$$\mathrm{HSA + NphOAc} \underset{k_{-1}}{\overset{k_{+1}}{\rightleftharpoons}} \mathrm{HSA{:}NphOAc} \underset{k_{-2}}{\overset{k_{+2}}{\rightleftharpoons}} \mathrm{HSA\text{-}OAc} \overset{k_{+3}}{\rightleftharpoons} \mathrm{HSA + AcOH}$$

$$+ \mathrm{NphOH} \quad k_{-3}$$

Scheme 1.

3. Results and discussion

The determination of kinetic parameters of Scheme 1 is simplified by the fact that the formation of the HSA:NphOAc complex from HSA and NphOAc may be regarded as being at equilibrium throughout the reaction (*i.e.*, $k_{-1} >> k_{+2}$; see Scheme 1). This pseudo-first-order process is characterized by the rate constant k_1^{obs} given by Eq. (1):

$$k_1^{obs} = k_{+1} \times [\mathrm{HSA}] + k_{-1} \quad (1)$$

Evidence for this is based on the observation that under all the present experimental conditions no lag phase occurs in the release of NphOH from NphOAc in the presence of HSA (see Fig. 1). This means that the equilibration of HSA:NphOAc with HSA and NphOAc is complete within 1.1 ms (*i.e.*, the "dead-time" of the rapid-mixing stopped-flow apparatus), therefore $k_1^{obs} \geqslant 3.5 \times 10^3\ s^{-1}$. Given that values of K_s ($=k_{-1}/k_{+1}$) for NphOAc binding to HSA range between 6.6×10^{-5} M and 5.1×10^{-4} M (see Table 1), it follows that $k_{-1} \geqslant 3.5 \times 10^3\ s^{-1}$ and $k_{+1} \geqslant 6.8 \times 10^6\ M^{-1}\ s^{-1}$; therefore, since values of k_{+2} range between $8.2 \times 10^{-3}\ s^{-1}$ and $2.1\ s^{-1}$ (see Table 1), the prediction $k_{-1} >> k_{+2}$ is satisfied. A further simplifying condition arises from the observation that the rate of NphOH release from NphOAc catalyzed by HSA is unaffected by the addition of NphOH (up to 1.0×10^{-4} M) in the reaction mixtures, therefore values of k_{-2} and k_{-3} are very low, becoming indistinguinshable from $0\ s^{-1}$. As a whole, the formation of the HSA:NphOAc complex from HSA and NphOAc can be treated as a rapid equilibrium process.

When [HSA] ⩾ 5×[NphOAc] and $k_{-1} >> k_{+2}$, the rate of NphOH release from NphOAc should be a first-order process with a pseudo-first-order rate constant (*i.e.*, k_{app}), according to Eq. (2):

$$k_{app} = (k_{+2} \times [\mathrm{HSA}])/(K_s + [\mathrm{HSA}]) \quad (2)$$

The reaction of HSA with NphOAc is a first-order process for more than 95% of its course (Fig. 1, panel A) and values of k_{app} are independent of the observation wavelength over the whole range explored (*i.e.*, between 350 and 450 nm) at fixed NphOAc concentration. Moreover, values of k_{app} are independent of the NphOAc concentration when [HSA] ⩾ 5×[NphOAc]. Values of k_{+2} and K_s (see Table 1) were determined by Eq. (2) from hyperbolic plots of k_{app} *versus* [HSA], as shown in Fig. 1 (panel B).

When [NphOAc] ⩾ 5×[HSA], a mono-exponential time course preceding the apparent very slow pseudo-steady-state process occurs (Fig. 1, panel C). When $k_{+2} \geqslant 5 \times k_{+3}$, the differential equations arising from Scheme 1 may be solved [14] to describe the time course of NphOH release in the early stages of the reaction. The resulting expression is given in Eqs. (3)–(5):

$$[\mathrm{NphOH}] = \{(k_{cat} \times [\mathrm{HSA}] \times [\mathrm{NphOAc}] \times t)/(K_m + [\mathrm{NphOAc}])\} + \alpha \times [\mathrm{HSA}] \times (1 - e^{-kt}) \quad (3)$$

where

$$\alpha = \{(k_{+2} \times [\mathrm{NphOAc}])/((k_{+2} + k_{+3}) \times (K_m + [\mathrm{NphOAc}]))\}^2 \quad (4)$$

and

$$k_{obs} = (k_{+2} \times [\mathrm{NphOAc}])/(K_s + [\mathrm{NphOAc}]) + k_{+3} \quad (5)$$

As predicted from Eqs. (3)–(5), a "burst" phase of NphOH release of amplitude α×[HSA] with the first-order rate constant k_{obs} occurs at all pH values explored. Values of α, obtained at [NphOAc] ⩾ 5×[HSA], range between 0.97 and 1.03, the average α value is 1.00 ± 0.03. This indicates that the HSA:NphOAc:NphOH stoichiometry is 1:1:1. Moreover, the time course of the "burst" phase of NphOH release is a first-order process for more than 95% of its course and values of k_{obs} are independent of the observation wavelength over the whole range explored (*i.e.*,

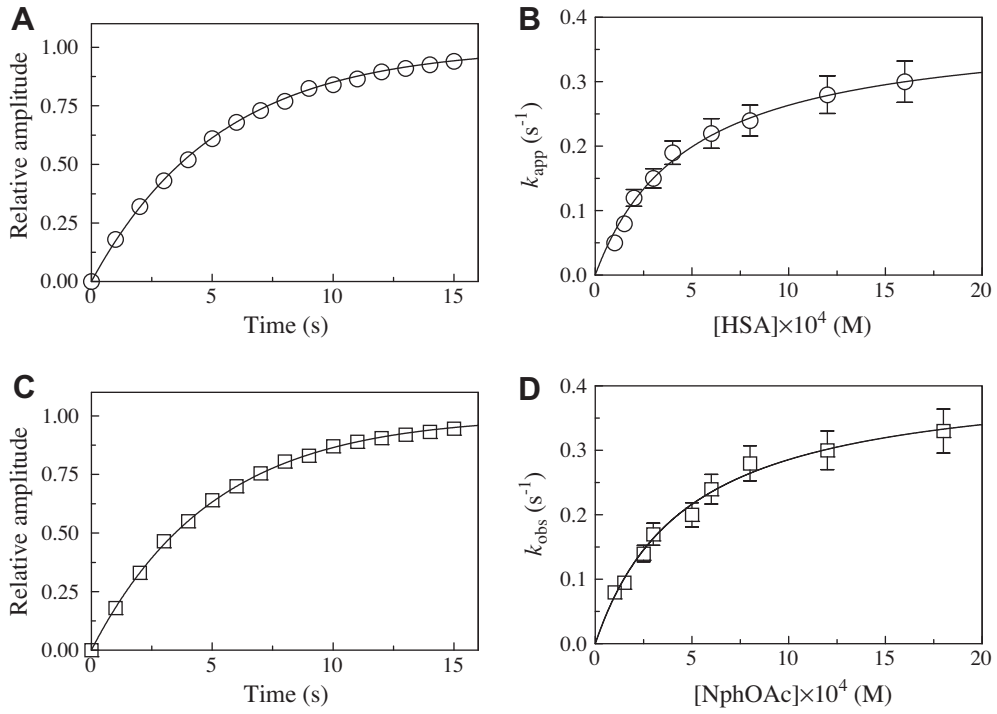

Fig. 1. HSA-mediated hydrolysis of NphOAc, at pH 7.5 and 22.0 °C. Panel A. Time course of the reaction of 2.0×10^{-5} M NphOAc with 4.0×10^{-4} M HSA, *i.e.* [HSA] ⩾ 5×[NphOAc]. The continuous line was calculated according to the following equation: $[NphOAc]_t = [NphOAc]_i \times (1-e^{-kapp \times t})$ with $k_{app} = (1.8 \pm 0.2) \times 10^{-1}$ s^{-1}. Panel B. Dependence of k_{app} on the HSA concentration at [HSA] ⩾ 5×[NphOAc]. The continuous line was obtained according to Eq. (2) with the following parameters $k_{+2} = (3.9 \pm 0.4) \times 10^{-1}$ s^{-1} and $K_s = (4.8 \pm 0.5) \times 10^{-4}$ M. [NphOAc] was 2.0×10^{-5} M and [HSA] ranged between 1.0×10^{-4} M and 1.6×10^{-3} M. Panel C. Time course of the reaction of 2.0×10^{-5} M HSA with 5.0×10^{-4} M NphOAc, *i.e.* [NphOAc] ⩾ 5×[HSA]. The continuous line was calculated according to the following equation: $[NphOAc]_t = [NphOAc]_i \times (1-e^{-kobs \times t})$ with $k_{obs} = (2.0 \pm 0.2) \times 10^{-1}$ s^{-1}. Panel D. Dependence of k_{obs} on the HSA concentration at [NphOAc] ⩾ 5×[HSA]. The continuous line was obtained according to Eq. (5) with the following parameters $k_{+2} = (4.2 \pm 0.4) \times 10^{-1}$ s^{-1} and $K_s = (4.7 \pm 0.5) \times 10^{-4}$ M. The value of k_{+3} approximates to 0 s^{-1}. [HSA] was 2.0×10^{-5} M, and [NphOAc] ranged between 1.0×10^{-4} M and 1.8×10^{-3} M. For details, see text.

Table 1
Values of catalytic parameters for the HSA-catalyzed hydrolysis of NphOAc, at 22.0 °C.

pH	[HSA] ⩾ 5×[NphOAc]			[NphOAc] ⩾ 5×[HSA]		
	K_s (M)	k_{+2} (s^{-1})	k_{+2}/K_s (M^{-1} s^{-1})	K_s (M)	k_{+2} (s^{-1})	k_{+2}/K_s (M^{-1} s^{-1})
5.8	$(4.3 \pm 0.4) \times 10^{-4}$	$(8.2 \pm 0.8) \times 10^{-3}$	$(1.9 \pm 0.2) \times 10^{1}$	$(5.1 \pm 0.5) \times 10^{-4}$	$(8.4 \pm 0.8) \times 10^{-3}$	$(1.7 \pm 0.2) \times 10^{1}$
6.8	$(5.0 \pm 0.5) \times 10^{-4}$	$(1.1 \pm 0.1) \times 10^{-1}$	$(2.2 \pm 0.2) \times 10^{2}$	$(4.8 \pm 0.5) \times 10^{-4}$	$(1.0 \pm 0.1) \times 10^{-1}$	$(2.0 \pm 0.2) \times 10^{2}$
7.5	$(4.8 \pm 0.5) \times 10^{-4}$	$(3.9 \pm 0.4) \times 10^{-1}$	$(8.1 \pm 0.9) \times 10^{2}$	$(4.7 \pm 0.5) \times 10^{-4}$	$(4.2 \pm 0.4) \times 10^{-1}$	$(8.4 \pm 0.9) \times 10^{2}$
8.0	$(2.9 \pm 0.3) \times 10^{-4}$	$(8.9 \pm 0.9) \times 10^{-1}$	$(3.1 \pm 0.3) \times 10^{3}$	$(3.1 \pm 0.3) \times 10^{-4}$	$(8.5 \pm 0.8) \times 10^{-1}$	$(3.0 \pm 0.3) \times 10^{3}$
8.6	$(1.5 \pm 0.2) \times 10^{-4}$	1.5 ± 0.1	$(9.9 \pm 1.0) \times 10^{3}$	$(1.3 \pm 0.1) \times 10^{-4}$	1.4 ± 0.1	$(9.6 \pm 0.9) \times 10^{3}$
9.0	$(1.1 \pm 0.1) \times 10^{-4}$	1.9 ± 0.2	$(1.7 \pm 0.2) \times 10^{4}$	$(1.0 \pm 0.1) \times 10^{-4}$	2.1 ± 0.2	$(1.9 \pm 0.2) \times 10^{4}$
9.6	$(7.7 \pm 0.8) \times 10^{-5}$	2.1 ± 0.2	$(2.7 \pm 0.3) \times 10^{4}$	$(7.5 \pm 0.7) \times 10^{-5}$	1.9 ± 0.2	$(2.8 \pm 0.3) \times 10^{4}$
10.2	$(6.6 \pm 0.7) \times 10^{-5}$	2.0 ± 0.2	$(3.2 \pm 0.3) \times 10^{4}$	$(6.8 \pm 0.7) \times 10^{-5}$	2.1 ± 0.2	$(3.1 \pm 0.3) \times 10^{4}$

between 350 and 450 nm) at fixed HSA concentration. Values of k_{obs} are independent of the HSA concentration when [NphOAc] ⩾ 5×[HSA]. Values of k_{+2} and K_s (see Table 1) were determined by Eq. (5) from hyperbolic plots of k_{obs} *versus* [S], as shown in Fig. 1 (panel D). Under all the experimental conditions, the *y*-intercept of the hyperbola described by Eq. (5) approximates to 0 s^{-1}, thus indicating that the value of k_{+3} is at least 100-fold smaller than the k_{obs} value obtained at the lowest NphOAc concentration (*i.e.*, $k_{+3} < 10^{-5}$ s^{-1}). Accordingly, k_{+3} for Tyr411-OAc deacylation corresponds to 3.2×10^{-6} s^{-1}, at pH 8.0 and 22.0 °C [8].

As predicted by Scheme 1, values of K_s and k_{+2} obtained under conditions where [HSA] ⩾ 5×[NphOAc] from Eq. (2) are in excellent agreement with those obtained under conditions where [NphOAc] ⩾ 5×[HSA] from Eq. (5) (see Table 1). Moreover, data here reported indicate that the deacylation process is rate limiting in the HSA-catalyzed hydrolysis of NphOAc (*i.e.*, $k_{+3} << k_{+2}$). Lastly, values of K_s and k_{+2} here obtained are in agreement with those previously reported [12,13].

Accounting for values of $K_s = 2.9 \times 10^{-4}$ M (present study), $k_{+2} = 8.9 \times 10^{-1}$ s^{-1} (present study), and $k_{+3} = 3.2 \times 10^{-6}$ s^{-1} [8], values of K_m ($\cong 1 \times 10^{-9}$ M) and k_{cat} ($\cong 3 \times 10^{-6}$ s^{-1}) for the HSA-catalyzed hydrolysis of NphOAc have been estimated at pH 8.0 and 22.0 °C, according to Eqs. (6) and (7):

$$K_m = (K_s \times k_{+3})/(k_{+2} + k_{+3}) \quad (6)$$

$$k_{cat} = (k_{+2} \times k_{+3})/(k_{+2} + k_{+3}) \quad (7)$$

Notably, values of K_m and k_{cat} for the HSA-catalyzed hydrolysis of NphOAc cannot be determined experimentally since during the very low turnover (*i.e.*, $k_{cat} \cong 3 \times 10^{-6}$ s^{-1}) 81 amino-acid residues undergo acetylation, under conditions where [NphOAc] >> [HSA] [8].

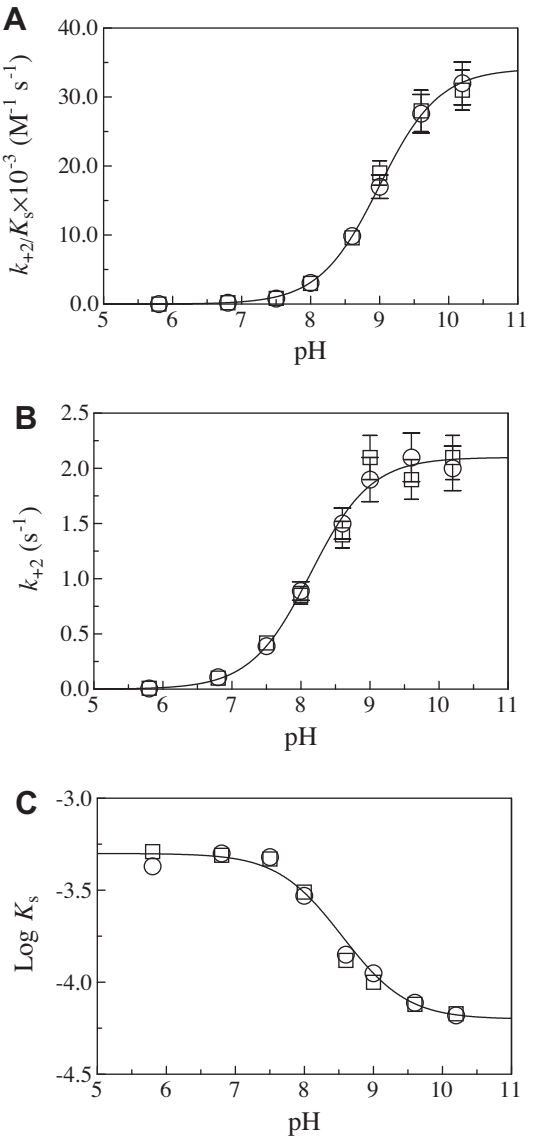

Fig. 2. pH-dependence of k_{+2}/K_s (panel A), k_{+2} (panel B), and K_s (panel C) for HSA-Tyr411-mediated hydrolysis of NphOAc, at 22.0 °C. Circles and squares indicate data obtained under conditions where [HSA] ⩾ 5×[NphOAc] and [NphOAc] ⩾ 5×[HSA], respectively. The continuous lines were obtained according to Eqs. (8)–(10) with the following parameters: panel A - $pK_{unl} = 9.0 \pm 0.1$ and $(k_{+2}/K_s)^{lim} = (3.4 \pm 0.4) \times 10^4$ M^{-1} s^{-1}; panel B - $pK_{lig} = 8.1 \pm 0.1$ and $k_{+2}^{lim} = 2.1 \pm 0.2$ s^{-1}; and panel C - $pK_{unl} = 9.0 \pm 0.1$, $pK_{lig} = 8.1 \pm 0.1$, and $K_s^{lim} = (6.6 \pm 0.7) \times 10^{-5}$ M. For details, see text.

Fig. 2 shows the pH-dependence of k_{+2}/K_s, k_{+2}, and K_s values for the HSA-catalyzed hydrolysis of NphOAc. Values of kinetic parameters obtained using different buffers at overlapping pH values match each other within the experimental error. Values of pK_a modulating the pH-dependence of k_{+2}/K_s, k_{+2}, and K_s were determined by data analysis according to Eqs. (8)–(10):

$$\mathrm{Log}K_s = -\mathrm{Log}K_s^{lim} + \mathrm{Log}((10^{-pH} + 10^{-pKunl})/(10^{-pH} + 10^{-pKlig})) \quad (8)$$

$$k_{+2} = k_{+2}^{lim}/(1 + (10^{-pH}/10^{-pKlig})) \quad (9)$$

$$k_{+2}/K_s = (k_{+2}/K_s)^{lim}/(1 + (10^{-pH}/10^{-pKunl})) \quad (10)$$

where K_s^{lim}, k_2^{lim}, and $(k_{+2}/K_s)^{lim}$ are the alkaline asymptotes of K_s, k_{+2}, and k_{+2}/K_s.

According to linked functions [14–16], the pH-dependence of k_{+2}/K_s and k_{+2} reflects the acid–base equilibrium of a single amino-acid residue in the substrate-free HSA (*i.e.*, $pK_{unl} = 9.0 \pm 0.1$) and in the HSA:NphOAc complex (*i.e.*, $pK_{lig} = 8.1 \pm 0.1$), respectively. Moreover, the pH-dependence of K_s reflects the acidic pK_a shift of a single amino-acid residue from the substrate-free HSA (*i.e.*, $pK_{unl} = 9.0 \pm 0.1$) to the HSA:NphOAc complex (*i.e.*, $pK_{lig} = 8.1 \pm 0.1$). The pK_{unl} value here reported is in agreement with that given in the literature [12,13]. As expected, the pK_{unl} value is substrate-independent (see present study and [17]); on the other hand, the pK_{lig} value depends on the chemical structure of the substrate (see present study and [17]), reflecting the different solvent accessibility of the ionization group(s) modulating catalysis.

The acidic pK_a shift of an apparently single ionizable side chain group of HSA upon NphOAc binding could reflect the reduced solvent accessibility of Tyr411, representing the primary esterase site of HSA (see [8,13,17]), although long range effects could not be excluded.

Tyr 411 is located in the FA3-FA4 cleft that is made of a mainly apolar region forming the FA3 site and a polar patch contributing the FA4 site. The polar patch is centered on Tyr411 and includes Arg410, Lys414, and Ser489 [5,15]. The analysis of the three-dimensional structure of the ligand-free HSA [19] and of the molecular model of the HSA:4-nitrophenyl propionate complex [13] suggests that the observed pH effects (Fig. 2) could reflect the acidic pK_a shift of Tyr411. This would render more stable the negative charge on the phenoxyl oxygen atom of Tyr411, which indeed appears to form a hydrogen bond with the carbonyl oxygen atom of 4-nitrophenyl propionate [13], potentiating its nucleophilic role as an electron donor in the pseudo-esterase activity of HSA.

In order to highlight the role of Tyr411, located in the FA3-FA4 cleft [18], as the primary esterase site for the HSA-catalyzed hydrolysis of NphOAc [8,13,17], the inhibitory effect of diazepam has been investigated under conditions where [NphOAc] > [HSA]. In fact, diazepam binds at the center of the FA3-FA4 cleft with one oxygen atom interacting with the hydroxyl group of Tyr411 [18]. As expected for the pure competitive inhibition mechanism [20], values of K_s for the HSA-catalyzed hydrolysis of NphOAc increase with the diazepam concentration (*i.e.*, [I]; Fig. 3), whereas values of k_{+2} are unaffected by the drug. The analysis of the linear dependence of the K_s^{app}/K_s ratio on the diazepam concentration (*i.e.*, [I]) according to Eq. (11):

$$K_s^{app}/K_s = [I]/K_I + 1 \quad (11)$$

allowed to determine the value of the equilibrium constant for diazepam binding to HSA (*i.e.*, K_I, corresponding to the absolute value of

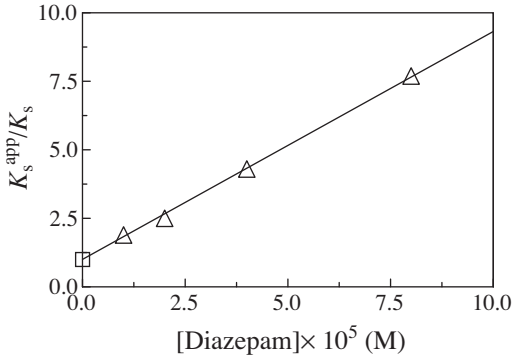

Fig. 3. Competitive inhibitory effect of diazepam on the HSA-catalyzed hydrolysis of NphOAc, at pH 7.5 and 22.0 °C. Data were obtained under conditions where [NphOAc] > [HSA]. The continuous line was obtained according to Eq. (11) with $K_I = 1.2 \times 10^{-5}$ M. For details, see text.

the x intercept of the linear plot). The value of K_I here determined agrees with that reported previously [17,21]. These data agree with the view that Tyr411 located at the FA3-FA4 cleft [18] is the primary esterase site for the HSA-catalyzed hydrolysis of NphOAc [8,13].

4. Conclusion

The reaction of NphOAc with HSA is reminiscent of that observed for acylating agents with other proteins (*e.g.*, cysteine and serine proteinases) [14,22]. However, the HSA-catalyzed hydrolysis of NphOAc is the result of the irreversible acetylation of 82 residues rather than of turnover [8]. Remarkably, the reaction of Tyr411 with NphOAc proceeds much faster than that catalyzed by any other amino-acid side chain of HSA [8,13].

Present data support the following considerations: (i) The hydrolysis of NphOAc by Tyr411, *i.e.* the most reactive group of HSA, appears to involve strong reversible binding prior to reaction. (ii) NphOAc acts as a suicide substrate, the value of the deacylation rate constant (*i.e.*, k_{+3}) being lower by several orders of magnitude than that of the acylation rate constant (*i.e.*, k_{+2}). (iii) The hydrolysis of NphOAc by HSA is inhibited competitively by diazepam, since both the substrate and the drug interact with Tyr411 at the FA3-FA4 cleft. (iv) The ionization state of Tyr411 modulates NphOAc hydrolysis; indeed substrate binding to HSA induces the acidic pK_a shift of the Tyr411 residue. (v) HSA acylation appears relevant from the pharmacokinetic viewpoint; indeed HSA acylation by aspirin [23], beside increasing the affinity of phenylbutazone and inhibiting bilirubin binding, reduces prostaglandin affinity, accelerating the clearance of prostaglandins and serving as an additional mechanism of the aspirin anti-inflammatory effect [24].

Acknowledgments

This work was partially supported by a grant from Ministero dell'Istruzione, dell'Università e della Ricerca of Italy (Università Roma Tre, Roma, Italy; CLAR 2011 to P.A.).

References

[1] T. Peters Jr. (Ed.), All about Albumin: Biochemistry, Academic Press, San Diego and London, Genetics and Medical Applications, 1996.
[2] S. Curry, Beyond expansion: structural studies on the transport roles of human serum albumin, Vox Sang 83 (Suppl. 1) (2002) 315–319.
[3] M. Fasano, S. Curry, E. Terreno, M. Galliano, G. Fanali, P. Narciso, S. Notari, P. Ascenzi, The extraordinary ligand binding properties of human serum albumin, IUBMB Life 57 (2005) 787–796.
[4] R.L. Gundry, Q. Fu, C.A. Jelinek, J.E. Van Eyk, R.J. Cotter, Investigation of an albumin-enriched fraction of human serum and its albuminome, Proteomics Clin. Appl. 1 (2007) 73–88.
[5] S. Curry, Lessons from the crystallographic analysis of small molecule binding to human serum albumin, Drug Metab. Pharmacokinet. 24 (2009) 342–357.
[6] G. Fanali, A. di Masi, V. Trezza, M. Marino, M. Fasano, P. Ascenzi, Human serum albumin: from bench to bedside, Mol. Aspects Med. 33 (2012) 209–290.
[7] K. Honma, M. Nakamura, Y. Ishikawa, Acetylsalicylate-human serum albumin interaction as studied by NMR spectroscopy-antigenicity-producing mechanism of acetylsalicylic acid, Mol. Immunol. 28 (1991) 107–113.
[8] O. Lockridge, W. Xue, A. Gaydess, H. Grigoryan, S.J. Ding, L.M. Schopfer, S.H. Hinrichs, P. Masson, Pseudo-esterase activity of human albumin: slow turnover on tyrosine 411 and stable acetylation of 82 residues including 59 lysines, J. Biol. Chem. 283 (2008) 22582–22590.
[9] R.F. Chen, Removal of fatty acids from serum albumin by charcoal treatment, J. Biol. Chem. 242 (1967) 173–181.
[10] M. Sogami, J.F. Foster, Isomerization reactions of charcoal-defatted bovine plasma albumin. The N–F transition and acid expansion, Biochemistry 7 (1968) 2172–2182.
[11] J. Cabrera-Crespo, V.M. Goncalves, E.A. Martins, S. Grellet, A.P. Lopes, I. Raw, Albumin purification from human placenta, Biotechnol. Appl. Biochem. 31 (2000) 101–106.
[12] G.E. Means, M.L. Bender, Acetylation of human serum albumin by *p*-nitrophenyl acetate, Biochemistry 14 (1975) 4989–4994.
[13] Y. Sakurai, S.F. Ma, H. Watanabe, N. Yamaotsu, S. Hirono, Y. Kurono, U. Kragh-Hansen, M. Otagiri, Esterase-like activity of serum albumin: characterization of its structural chemistry using *p*-nitrophenyl esters as substrates, Pharm. Res. 21 (2004) 285–292.
[14] M.R. Hollaway, E. Antonini, M. Brunori, The pH-dependence of rates of individual steps in ficin catalysis, Eur. J. Biochem. 24 (1971) 332–341.
[15] E. Antonini, P. Ascenzi, The mechanism of trypsin catalysis at low pH: proposal for a structural model, J. Biol. Chem. 256 (1981) 12449–12455.
[16] L. Peller, R.A. Alberty, Multiple intermediates in steady state enzyme kinetics: I. The mechanism involving a single substrate and product, J. Am. Chem. Soc. 81 (1959) 5907–5914.
[17] P. Ascenzi, M. Fasano, Pseudo-enzymatic hydrolysis of 4-nitrophenyl myristate by human serum albumin, Biochem. Biophys. Res. Commun. 422 (2012) 219–223.
[18] J. Ghuman, P.A. Zunszain, I. Petitpas, A.A. Bhattacharya, M. Otagiri, S. Curry, Structural basis of the drug-binding specificity of human serum albumin, J. Mol. Biol. 353 (2005) 38–52.
[19] S. Sugio, A. Kashima, S. Mochizuki, M. Noda, K. Kobayashi, Crystal structure of human serum albumin at 2.5 Å resolution, Protein Eng. 12 (1999) 439–446.
[20] P. Ascenzi, M.G. Ascenzi, G. Amiconi, Enzyme competitive inhibition. Graphical determination of K_i and presentation of data in comparative studies, Biochem. Mol. Biol. Edu. 15 (1987) 134–135.
[21] G. Fanali, Y. Cao, P. Ascenzi, V. Trezza, T. Rubino, D. Parolaro, M. Fasano, Binding of δ9-tetrahydrocannabinol and diazepam to human serum albumin, IUBMB Life 63 (2011) 446–451.
[22] F.J. Kezdy, M.L. Bender, The kinetics of the α-chymotrypsin-catalyzed hydrolysis of p-nitrophenyl acetate, Biochemistry 1 (1962) 1097–1106.
[23] F. Yang, C. Bian, L. Zhu, G. Zhao, Z. Huang, M. Huang, Effect of human serum albumin on drug metabolism: structural evidence of esterase activity of human serum albumin, J. Struct. Biol. 157 (2007) 348–355.
[24] M.S. Liyasova, L.M. Schopfer, O. Lockridge, Reaction of human albumin with aspirin *in vitro*: mass spectrometric identification of acetylated lysines 199, 402, 519, and 545, Biochem. Pharmacol. 79 (2010) 784–791.